Tumor-Imaging Potential of Liposomes Loaded with In-111-NTA: Biodistribution in Mice

Richard T. Proffitt, Lawrence E. Williams, Cary A. Presant, George W. Tin, Joseph A. Uliana, Ronald C. Gamble, and John D. Baldeschwieler

City of Hope National Medical Center, Duarte, Vestar Research, Inc., Pasadena, California Institute of Technology, Pasadena, and Wilshire Oncology Medical Group, Los Angeles, California

EMT6 tumors in BALB/c mice have been successfully imaged with small (<0.1μ), unilamellar lipid vesicles (SUVs) loaded with In-111 nitrilotriacetic acid (In-111 NTA). Neutral SUVs prepared from distearoyl phosphatidylcholine (DSPC) and cholesterol (CH) (ratio 2:1) delivered sufficient radioactivity to allow tumor visualization 24 hr after i.v. injection; so did positively and negatively charged SUVs with the ratio 4:1:1 for DSPC:CH:X, where X was stearylamine or dicetyl phosphate. Other SUVs containing a 6-aminomannose or 6-aminomannitol derivative of cholesterol did not cause significant tumor accumulation of In-111 NTA, and tumor images were not readily discernible. The maximum tumor-associated radioactivity, 18.5% of injected dose per gram of tissue, was achieved with neutral SUVs. This level of tumor-associated In-111 was over 4 times that observed when unencapsulated In-111 NTA was injected. Neutral SUVs also gave the lowest specific activities in the liver and spleen (14.6% and 18.8% of dose respectively).

J Nucl Med 24: 45–51, 1983

Numerous investigators have described the use of liposomes as carriers to protect and deliver therapeutic or diagnostic agents (for reviews see Refs. *1–3*). Previous work in our laboratories has demonstrated that small, unilamellar, lipid vesicles (SUVs) can be prepared from pure phospholipids, cholesterol, and a 6-aminomannose derivative of cholesterol. These SUVs have unusual properties in vivo (*4–6*), and were shown to have a high affinity for murine EMT6 tumor cells in vitro (*7*). Since methods have been developed for efficiently incorporating chelated In-111 into these SUVs (*8*), we undertook this study to investigate the potential of In-111-loaded SUVs for tumor imaging in vivo.

Several earlier in vivo animal studies used liposomes as tumor-imaging agents, and were able to demonstrate some degree of enhanced localization of radiotracer in tumor (*9–12*). Of these studies, the best tumor uptake of radiotracer was observed with negatively charged liposomes prepared with egg lecithin (*9*). In the present study, we describe the use of SUVs prepared from pure distearoyl phosphatidylcholine and cholesterol, which are relatively stable to lysis in vivo (*5,13*). Furthermore, we have used the weak chelator, nitrilotriacetic acid (NTA), which can be displaced by proteins and allows the In-111 to remain at the site of liposome lysis. Thus In-111 accumulates in tissues over a relatively long time after liposome injection.

MATERIALS AND METHODS

Liposome preparation. SUVs containing the ionophore A23187 were prepared from distearoyl phosphatidylcholine (DSPC), cholesterol (CH), dicetyl phosphate (DP), stearylamine (SA), and the 6-aminomannose (AM) and 6-aminomannitol (AML) derivatives of

Received Apr. 12, 1982; revision accepted Sept. 21, 1982.

For reprints contact: Richard T. Proffitt, PhD, Dept. of Med. Oncology, City of Hope National Med. Ctr., 1500 E. Duarte Rd., Duarte, CA 91010.

cholesterol (*15,16*) according to the method of Mauk et al. (*8,13*). Briefly, chloroform solutions of lipid mixtures (with the following mole ratios: DSPC:CH = 2:1, DSPC:CH:X = 4:1:1 (where X = SA, DP, AM, or AML); and DSPC:CH:AM = 8:3:1) were evaporated to dryness under N_2 and further dried under vacuum overnight. To each tube was added 0.6 ml 10 m*M* potassium phosphate in 0.9% NaCl, pH 7.4 (PBS), containing 1 m*M* NTA, and the contents were vortexed briefly. The suspension was sonicated at 100 W for 5 min under a nitrogen atmosphere, using a probe sonicator equipped with a titanium microtip. SUVs were annealed at 60°C for 10 min and then centrifuged at 400 *g*. Unencapsulated NTA was removed from SUVs by filtering the mixture through a 30- by 1.5-cm Sephadex G-50 column. Liposome size was determined by electron microscopy of preparations negatively stained with uranyl acetate.

In-111 loading procedure. Loading of In-111 into preformed SUVs was facilitated by the presence of the divalent cation ionophore A23187 (*17,18*) in the lipid bilayer. The loading was performed by incubation at 60–80° for 30 to 60 min (*8*). Incubations were terminated by the addition of 10 m*M* EDTA in PBS, and free In-111 was separated from the loaded liposomes by gel filtration on a Sephadex G-50 column. Up to 90% of the added In-111 could be incorporated into preformed liposomes by this method, and specific activities of up to 300 μCi/mg lipid have been reported (*13*).

EMT6 tumor growth. EMT6 tumor cells were obtained from Dr. Robert Klevecz at City of Hope Research Institute. Male BALB/c mice weighing 20–25 g were injected s.c. on the right hind leg with 500,000 EMT6 cells (*19*) in 0.1 ml sterile PBS. Tumors were allowed to grow for 10–20 days before these animals were used for imaging studies. At this stage, tumors weighed between 0.1 and 0.6 g. One to 2 mg SUVs, loaded with a total activity of up to 30 μCi In-111, were injected into the tail vein of each animal. Control animals were injected with unencapsulated In-111 NTA or I-131 albumin.

Gamma imaging. Within one hr or 24 hr after injection, each animal was anesthetized with 40 mg/Kg sodium pentobarbital and positioned on a platform 12 cm from the gamma scintillation camera equipped with a 6-mm pinhole. Whole-body dorsal images were recorded on x-ray film, and the corresponding digitized data were stored on magnetic disc for subsequent computer analysis.

Biodistribution of radioactivity. Immediately after the 1-hr or 24-hr images were acquired, animals were killed and dissected to determine the organ distribution of radioactivity. Organs or tissues were excised, washed in PBS, blotted dry, and weighed. Radioactivity was measured in a well gamma spectrometer and quantitated based on activity of In-111 injected in vivo.

RESULTS

Electron micrographs of each liposome composition confirmed that SUVs were actually being formed by the described procedure. All preparations examined had a heterogeneous size distribution with a mean diameter of less than 65 nm. The smallest mean diameter observed was 53 nm in neutral DSPC:CH SUV preparations.

Figure 1 shows whole-body scintigraphs of tumor-bearing mice that had been injected with free or SUV-entrapped In-111 NTA 24 hr previously. EMT6 tumor images are clearly discernible in animals injected with neutral (DSPC:CH), negative (DSPC:CH:DP), and positive (DSPC:CH:SA) SUVs. Free In-111 NTA also produced faint tumor images, but was more uniformly

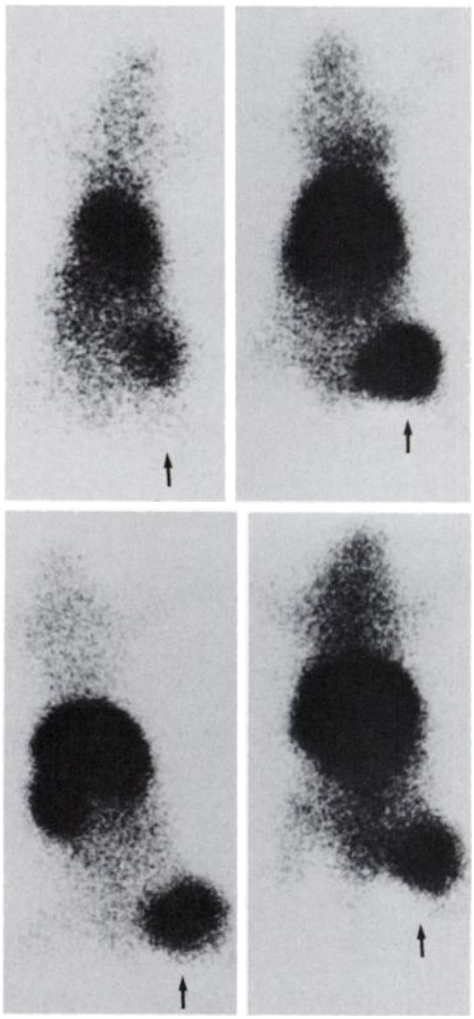

FIG. 1. Whole-body gamma camera images of mice bearing EMT6 tumors on right hind legs. Dorsal images of anesthesized mice were acquired 24 hr after i.v. injection of free or SUV-entrapped In-111 NTA. Arrow indicates tumor location in each image. Free In-111 NTA, 50,000 counts acquired (upper left). In-111 NTA entrapped in neutral SUVs (DSPC:CH = 2:1), 100,000 counts acquired (upper right). In-111 NTA entrapped in positive SUVs (DSPC:CH:SA = 4:1:1), 100,000 counts acquired (lower left). In-111 NTA entrapped in negative SUVs (DSPC:CH:DP = 4:1:1), 100,000 counts acquired (lower right).

TABLE 1. BIODISTRIBUTION OF RADIOACTIVITY IN MICE BEARING EMT6 TUMOR, AT 24 HR AFTER INJECTION OF FREE OR SUV-ENCAPSULATED In-111 NTA

		% Injected dose per gram of tissue*		
Organ	Free In-111 NTA (n = 5)†	In-111 NTA in neutral SUVs‡ (n = 6)†	In-111 NTA in positive SUVs‡ (n = 5)†	In-111 NTA in negative SUVs‡ (n = 4)†
Tumor	4.6 (2.3–7.3)	18.4 (14.0–23.4)	8.8 (6.0–13.8)	10.6 (6.6–14.2)
Blood	0.69 (0.28–1.1)	5.2 (4.3–8.0)	0.89 (0.67–1.2)	1.3 (0.90–1.6)
Liver	5.5 (2.8–10.1)	17.4 (12.9–16.6)	31.0 (26.4–35.5)	16.6 (14.7–18.0)
Spleen	5.1 (2.3–10.7)	20.6 (14.0–21.0)	41.2 (30.0–47.8)	39.3 (36.0–44.0)
Kidney	9.1 (7.0–11.5)	6.4 (5.1–7.7)	7.2 (6.9–7.4)	17.7 (13.1–21.4)
Lung	5.0 (2.3–10.7)	4.9 (4.2–7.9)	3.0 (2.8–4.5)	3.0 (2.3–3.4)
Bone	2.7 (2.4–3.4)	3.3 (2.9–6.2)	2.9 (2.2–5.2)	4.8 (4.1–5.3)
Muscle	0.75 (0.46–1.3)	1.2 (0.48–1.7)	0.74 (0.45–1.2)	1.1 (0.9–1.3)

* Mean value for mice in group; range in parentheses.
† n = number of mice in group.
‡ Liposome compositions expressed as molar ratios were: for neutral SUVs, DSPC:CH = 2:1; for positive SUVs, DSPC:CH:SA = 4:1:1; and for negative SUVs, DSPC:CH:DP = 4:1:1.

distributed throughout the animals' bodies. A comparison of the biodistributions of In-111 NTA in each of these vesicle types, and of free In-111 NTA, is presented in Table 1. Neutral SUVs provided the best delivery of In-111 to tumor tissue. The tumor's specific activity in this instance was at least 4 times that of the specific activity observed when free In-111 NTA was injected. In addition, the tumor's specific activity achieved with neutral SUVs was equal to, or greater than, the corresponding specific activities of liver and spleen, the usual organs that accumulate liposomes. It can also be seen in Table 1 that, as liver and spleen uptake of In-111 decreases, the activity remaining in blood increases. The increase in tumor-associated radioactivity generally correlates with the blood level of In-111.

Figure 2 shows images obtained within 1 hr of injection of free In-111 NTA and of In-111 NTA in neutral SUVs. In Figure 2 (left), free In-111 NTA can be seen accumulating in the bladder, but tumors located on the animals' right rear legs are not visualized. At this time, the percent injected dose of In-111 per gram of blood is 10.9 (n = 4) for free In-111 NTA and 45.1 (n = 5) for In-111 NTA in neutral SUVs. However, the tumor-to-blood ratios at the 1-hr time point were only 0.40 and 0.12, respectively. Clearly the level of radioactivity in the blood could make only a small contribution to the total radioactivity observed in the tumor.

As an additional control, I-131 albumin was administered i.v. to a group of tumor-bearing mice in order to determine the total contribution of a labeled blood-borne protein to the total tumor-associated radioactivity. Biodistribution data obtained 24 hr after injection of I-131 albumin showed that ratio of tumor-associated radioactivity to the level in blood was 0.70.

Since we had previously demonstrated a strong association of 6-aminomannose-derivatized SUVs (AM SUVs) with EMT6 tumor cells in vitro (*7*), we attempted tumor imaging with [In-111 NTA]AM SUVs. Our observations confirmed that a significant fraction of the AM SUVs (DSPC:CH:AM = 4:1:1) were arrested in the lungs within 1 hr after injection, and that most of the In-111 was ultimately deposited in the liver, as was described previously by Mauk et al. (*5*). Definitive tumor images would not be obtained with this agent, as is indicated by the low specific activity of the tumor (Table 2).

AM/2 SUVs (DSPC:CH:AM = 8:3:1) do not localize in the lung after injection, so it seemed reasonable to assume that [In-111 NTA]AM/2 SUVs might be better

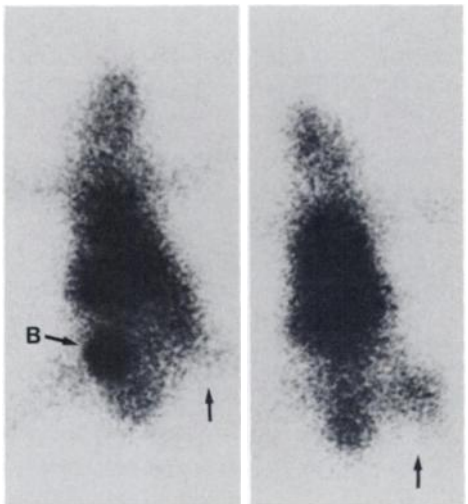

FIG. 2. Whole body dorsal images of mice bearing EMT6 tumor, scintigraphed 1 hr after i.v. injection of In-111 NTA, free or entrapped in DSPC:CH SUVs. Arrow indicates tumor location in each image. Free In-111 NTA, 60,000 counts acquired (left); B = bladder. In-111 NTA in neutral DSPC:CH SUVs, 100,000 counts acquired (right).

TABLE 2. BIODISTRIBUTION OF RADIOACTIVITY IN MICE BEARING EMT6 TUMOR, AT 24 HR AFTER I.V. ADMINISTRATION OF In-111 NTA ENCAPSULATED IN SYNTHETIC GLYCOLIPID-MODIFIED SUVs

	% Injected dose per gram of tissue*		
Organ	In-111 NTA in AM† (n = 2)‡	In-111 NTA in AM/2† (n = 3)‡	In-111 NTA in AML† (n = 3)‡
Tumor	0.91 (0.84–0.97)	1.0 (0.7–1.6)	1.7 (1.4–1.8)
Blood	0.23 (0.22–0.24)	0.24 (0.16–0.28)	0.30 (0.28–0.33)
Liver	29.6 (27.9–31.4)	40.5 (35.2–48.3)	17.4 (15.8–18.4)
Spleen	49.0 (42.3–55.8)	74.4 (50.8–106.2)	56.0 (43.6–64.0)
Kidney	4.6 (4.5–4.7)	2.5 (2.2–3.0)	6.5 (5.6–7.6)
Lung	3.2 (2.5–4.0)	1.5 (1.0–2.5)	4.7 (3.3–7.0)
Bone	1.7 (1.6–1.9)	1.2 (0.8–1.9)	3.0 (2.6–3.6)
Muscle	0.32 (0.28–0.37)	0.13(0.09–0.20)	0.36 (0.34–0.39)

* Mean value for animals in group, range in parentheses.

† Liposome molar ratio compositions were: for AM, DSPC:CH:AM = 4:1:1; AM/2, DSPC:CH:AM = 8:3:1; and for AML, DSPC:CH:AML = 4:1:1.

‡ n = number of mice per group.

tumor-imaging agents. Table 2 shows that this was not the case; in fact, AM/2 vesicles had a very high affinity for liver and spleen, and the blood level of radioactivity was very low. At 24 hr, the combined radioactivity in liver and spleen averaged greater than 75% of the total dose. This was the highest liver and spleen uptake of liposome-entrapped tracer that we observed with any of the liposome compositions studied.

Since positively charged liposomes bind to EMT6 cells in vitro to a much greater extent than either neutral or negatively charged liposomes (*7*), we investigated aminomannose lipid (AML), another synthetic glycolipid derivative with a positive charge. Compared with AM/2 SUVs, these AML SUVs did not show a lower affinity for liver and spleen (Table 2) and an increased uptake by tumor, but their level of tumor-associated radioactivity was still $1/3$ to $1/10$ of that observed in the experiments with the neutral or charged liposomes that did not contain synthetic glycolipid derivatives (Table 1).

DISCUSSION

We have shown that neutral, positive, and negative SUVs can deliver sufficient In-111 to EMT6 tumors to allow definitive delineation of tumors by gamma camera. Our biodistribution results with neutral DSPC:CH SUVs are similar to the biodistribution results obtained by Larson and coworkers (*20*) in mice bearing EMT6 tumor, injected with either Ga-67 citrate or Ga-67-labeled serum. Thus, 24 hr after injection, the best tumor-to-blood activity ratio reported by Larson et al. (*20*) was 4.3, while our average of tumor-to-blood ratio was 3.5. However, our observed specific activity in tumor was 18.4% injected dose per gram tumor with In-111-labeled neutral SUVs—nearly twice the tumor concentration reported for either Ga-67 citrate or Ga-67 labeled serum.

In previous attempts to enhance tumor accumulation of radionuclides by administering radiolabeled liposomes (*9–12*), the range of tumor-associated radioactivity was 1–7% injected dose per gram tumor. We have incorporated several improvements in liposome technique into this study, and we believe that one or more of these may account for the higher specific activities we have observed in tumors with some liposome preparations.

First, we have chosen liposome compositions that are known to resist leakage of liposome contents in vitro (*14*) and in vivo (*5*). These formulations include highly purified synthetic DSPC. It is generally recognized that naturally occurring phospholipid mixtures such as egg lecithin have broad, low gel-liquid crystalline-phase transition temperatures (T_c), whereas pure synthetic phospholipids with long fatty acyl chains have sharp, high T_cs (*21*). In addition, cholesterol has been included in all our liposome preparation studies, and this molecule is known to reduce liposome permeability both in vivo and in vitro (*22,23*).

Second, only small, sonicated liposomes were used in this study. Juliano and Stamp (*24*), and Abra and Hunt (*25*), have previously shown that small liposomes of any given lipid composition are cleared more slowly from circulation than an equivalent dose of large liposomes. Several studies have documented alterations in vascular permeability in tumors. For example, Underwood and Carr (*26*) found that Evans-blue-albumin complex leaked from vessels in a rat sarcoma at a faster rate than from normal tissues. However, leakage of colloidal carbon (30 nm diameter) at the tumor was observed only after administration of vasodilators. Likewise, Ackerman and Heckmer (*27*) observed that capillary permeability

was significantly greater in newly formed tumor vessels compared with the liver vasculature. We propose that the smallest liposomes in our preparations are capable of leaving the vascular bed at sites of increased capillary permeability, and thus account for the accumulation of In-111 in the tumor tissue. It is noteworthy that Richardson et al. (*12*) showed that small sonicated liposomes had seven-fold higher tumor uptake compared with larger liposomes produced in hand-shaken lipid suspensions.

Third, the effect of charge on the in vivo fate of liposomes should be considered. As Table 1 shows, neutral SUVs had the highest uptake in EMT6 tumors, followed by negative, and then positive SUVs. Although neutral SUVs had a slightly smaller average diameter, the difference in tumor uptake of these preparations could be ascribed primarily to the difference in surface charge on the various SUVs. However, two other results may also help to account for this observation. The first is that neutral SUVs of the same composition used in this study have been shown to have a greater stability in vivo than either the corresponding positive or negative SUVs (*5*). The second supporting observation is that the blood level of neutral SUVs was significantly higher than that of either positive or negative SUVs at 24 hr after injection (Table 2). This information further supports our hypothesis that intact liposomes that remain in circulation for long periods have a higher probability of accumulating at sites where vascular permeability is increased.

Although we have noted that increased tumor-associated radioactivity correlates with the increasing levels of blood-borne radioactivity, this increase is not directly due to the In-111 contained in the blood of the tumor. Comparisons of the tumor-to-blood ratios of In-111 specific activity support this statement. Thus, one hour after i.v. administration of In-111-labeled neutral SUVs, the tumor-to-blood radioactivity ratios is 0.12 and no tumor images are apparent (Fig. 2, right). The corresponding 24-hr ratio increased to 3.5 whereas the level of blood-borne tracer decreased from 45.1% to 5.2%, and distinct tumor images are obvious (Fig. 1, top right).

Likewise, we have compared free In-111 NTA distribution ratios at 1 hr and 24 hr. At 1 hr the ratio was low (0.40) and no tumor uptake could be seen (Fig. 2, left) although considerable In-111 is excreted as shown, by the prominent bladder image. Twenty-four hours after injection of free In-111 NTA, the tumor-to-blood ratio reached 6.7. However, this increase in tumor activity is probably due to binding of In-111 to transferrin (*28,29*), with subsequent localization of transferrin in the tumor by a mechanism analogous to that of Ga-67 localization in tumors (*30,31*).

In an additional attempt to define the contribution of blood-borne proteins to the total tumor radioactivity, we injected I-131 albumin into a series of mice bearing EMT6-tumor. After 24 hr, the blood level of I-131 was still 7.8% injected dose per gram blood, somewhat higher than the corresponding blood level of In-111 observed 24 hr after administration of neutral SUVs. However, the 24 hr tumor-to-blood ratio for I-131 was only 0.70, or ~1/5 of that observed with neutral SUV-encapsulated In-111. Clearly, blood levels of radioactivity make only minor contributions to the total activity found in tumor tissue.

By comparing the biodistribution of positive SA SUVs with those biodistributions determined for positive SUVs containing synthetic glycolipid derivatives (Table 2), one can see that factors other than liposomal surface charge must be considered to account for the observed differences. We hypothesize that interactions of plasma proteins with liposomes (*32*)—and possibly the rapid clearance of glycolipid-modified liposomes by cells with specific receptors for terminal sugars (*33,34*)—are factors that could contribute to the differences in biodistribution we have described.

A fourth factor that may contribute to the high levels of tumor radioactivity is the encapsulation of In-111 into liposomes as the NTA complex. NTA is a relatively weak chelator and, in the presence of serum, NTA can be displaced by transferrin and other proteins (*28,29*). Thus, when In-111 NTA is released from liposomes in vivo, the In-111 becomes tightly associated with surrounding proteins. If this release occurs on or within a cell, the In-111 remains fixed at that site. This occurrence provides two distinct advantages for the purposes of imaging. The first is that little radioactivity is lost due to renal excretion. After correcting for decay, we typically observed that more than 90% of the liposome-encapsulated radioactivity remained in the animal 24 hr after injection, based on the times required to accumulate a fixed number of counts with the gamma camera. A second advantage, as was pointed out by Espinola et al. (*35*), is that when a label remains fixed at the site of liposome destruction, one can obtain information on rate of liposome uptake by the tissue, as well as the total uptake. Thus, the high specific activities in tumor observed in this study are the result of a continuous accumulation of In-111 within the tumor over the entire 24-hr period. For comparison, [In-111 EDTA]SA SUVs were administered. EDTA is a strong chelate that cannot be displaced by proteins (*29*). In this case, specific activity in tumor was only 25% of the value found when liposomes were loaded with In-111 NTA (data not shown).

Finally, In-111 was loaded into preformed liposomes by the method of Mauk and Gamble (*8*). While this method is probably not essential for tumor imaging with liposomes, it does provide a highly efficient procedure for obtaining high In-111 specific activities in a relatively small liposome dose.

Based on the results presented in this communication,

we conclude that small liposomes are promising agents for the imaging of at least some tumors. Additional studies are now in progress to determine whether tumor localization of liposome-encapsulated radionuclides can be further enhanced, and to see if other tumor types can be successfully imaged with liposomes loaded with In-111 NTA.

ACKNOWLEDGMENT

This work was made possible in part by the Fred Marik Research Fund (RTP), a Cancer Center Seed Grant from the City of Hope National Medical Center (RTP), Grant #81-12589 from the National Science Foundation (JDB), Grant #GM21111-09 A1 from the National Institutes of Health (JDB), and by grants from the Monsanto Corp. and Merck & Co., Inc. (JDB).

The glycolipid derivatives of cholesterol were gifts from Dr. T. Y. Shen, Merck, Sharp, and Dohme Research Laboratories.

REFERENCES

1. GREGORIADIS G: The carrier potential of liposomes in biology and medicine. *N Engl J Med* 295:704-710, 765-770, 1976
2. KAYE SB: Liposomes—Problems and promise as selective drug carriers. *Cancer Treat Rev* 8:27-50, 1981
3. RYMAN BE, TYRRELL DA: Liposomes—Bags of potential. In *Essays in biochemistry*, Vol 16, Campbell PN, Marshall RD, Eds. London, Academic Press, 1980, pp 49-98
4. MAUK MR, GAMBLE RC, BALDESCHWIELER JD: Vesicle targeting: Timed release and specificity for leukocytes in mice by subcutaneous injection. *Science* 207:309-311, 1980
5. MAUK MR, GAMBLE RC, BALDESCHWIELER JD: Targeting of lipid vesicles: Specificity of carbohydrate receptor analogues for leukocytes in mice. *Proc Natl Acad Sci USA* 77:4430-4434, 1980
6. WU MS, ROBBINS JC, BUGIANESI RL, et al: Modified *in vivo* behavior of liposomes containing synthetic glycolipids. *Biochim Biophys Acta* 674:19-29, 1981
7. PROFFITT RT, PRESANT CA, ULIANA JA, et al: Preferential association in 6-aminomannose derivatized lipid vesicles with EMT6 tumor cells. *Proc Am Assoc Cancer Res* 22:41, 1981
8. MAUK MR, GAMBLE RC: Preparation of lipid vesicles containing high levels of entrapped radioactive cations. *Anal. Biochem* 94:302-307, 1979
9. DAPERGOLAS G, NEERUNJUN ED, GREGORIADIS G: Penetration of target areas in the rat by liposome-associated bleomycin, glucose oxidase and insulin. *FEBS Lett* 63: 235-239, 1976
10. NEERUNJUN ED, HUNT R, GREGORIADIS G: Fate of a liposome-associated agent injected into normal and tumour-bearing rodents: Attempts to improve localization in tumor tissue. *Biochem Soc Trans* 5:1380-1383, 1977
11. RICHARDSON VJ, JEYASINGH K, JEWKES RF, et al: Properties of [^{99m}Tc]technetium-labelled liposomes in normal and tumour-bearing rats. *Biochem Soc Trans* 5:290-291, 1977
12. RICHARDSON VJ, JEYASINGH K, JEWKES RF, et al: Possible tumor localization of Tc-99m-labeled liposomes: Effects of lipid composition, charge and liposome size. *J Nucl Med* 19:1049-1054, 1978
13. MAUK MR, GAMBLE RC: Stability of lipid vesicles in tissues of the mouse: A γ-ray perturbed angular correlation study. *Proc Natl Acad Sci USA* 76:765-769, 1979
14. HWANG KJ, MAUK MR: Fate of lipid vesicles *in vivo*: A gamma-ray perturbed angular correlation study. *Proc Natl Acad Sci USA* 74:4991-4995, 1977
15. CHABALA JC, SHEN TY: The preparation of 3-cholesteryl 6-(glycosylthio)hexyl ethers and their incorporation into liposomes. *Carbohydr Res* 67:55-63, 1978
16. PONPIPOM MM, BUGIANESI RL, SHEN TY: Cell surface carbohydrates for targeting studies. *Can J Chem* 58:214-220, 1980
17. REED PW, LARDY HA: A23187: A divalent cation Ionophore. *J Biol Chem* 247:6970-6977, 1972
18. PFEIFFER DR, REED PW, LARDY HA: Ultraviolet and fluorescent spectral properties of the divalent cation ionophore A23187 and its metal complexes. *Biochemistry* 13:4007-4014, 1974
19. ROCKWELL SC, KALLMAN RF, FAJARDO LF: Characteristics of a serially transplanted mouse mammary tumor and its tissue-culture adapted derivative. *J Natl Cancer Inst* 49: 735-749, 1972
20. LARSON SM, RASEY JS, ALLEN DR, et al: A transferrin-mediated uptake of Gallium-67 by EMT-6 sarcoma. II. Studies *in vivo* (BALB/c mice): Concise communication. *J Nucl Med* 20:843-846, 1979
21. PAGANO RE, WEINSTEIN JN: Interactions of liposomes with mammalian cells. *Ann Rev Biophys Bioeng* 7:435-468, 1978
22. POSTE G, PAPAHADJOPOULOS D, VAIL WJ: Lipid vesicles as carriers for introducing biologically active materials into cells. In *Methods in Cell Biology*, Vol 14. Prescott DM, Ed. New York, Academic Press. 1976. pp 33-71
23. KIRBY C, CLARKE J, GREGORIADIS G: Effect of the cholesterol content of small unilamellar liposomes on their stability *in vivo* and *in vitro*. *Biochem J* 186:591-598, 1980
24. JULIANO RL, STAMP D: The effect of particle size and charge on the clearance rates of liposomes and liposome encapsulated drugs. *Biochem Biophys Res Commun* 63:651-658, 1975
25. ABRA RM, HUNT CA: Liposome disposition *in vivo*. III. Dose and vesicle-size effects. *Biochim Biophys Acta* 666: 493-503, 1981
26. UNDERWOOD JCE, CARR I: The ultrastructure and permeability characteristics of the blood vessels of a transplantable rat sarcoma. *J Pathol* 107:157-166, 1972
27. ACKERMAN NB, HECHMER PA: Studies on the capillary permeability of experimental liver metastases. *Surg Gynecol Obst* 146:884-888, 1978
28. HOSAIN G, MCINTYRE PA, POULOSE K, et al: Binding of trace amounts of ionic indium-113m to plasma transferrin. *Clin Chim Acta* 24:69-75, 1969
29. GOODWIN DA, MEARES CF, SONG CH: The study of ^{111}In-labeled compounds in mice, using perturbed angular correlations of gamma radiations. *Radiology* 105:669-702, 1972
30. CLAUSEN J, EDELING C-J, FOGH J: ^{67}Ga binding to human serum proteins and tumor components. *Cancer Res* 34: 1931-1937, 1974
31. VALLABHAJOSULA SR, HARWIG JF, SIEMSEN JK, et al: Radiogallium localization in tumors: Blood binding and transport and the role of transferrin. *J Nucl Med* 21:650-656, 1980
32. BLACK CDV, GREGORIADIS G: Interaction of liposomes with blood plasma proteins. *Biochem Soc Trans* 4:253-256, 1976
33. SCHLESINGER PH, DOEBBER TW, MANDELL BF, et al:

Plasma clearance of glycoproteins with terminal mannose and N-acetylglucosamine by liver non-parenchymal cells. *Biochem J* 176:103-109, 1978

34. SHEPHERD VL, LEE YC, SCHLESINGER PH, et al: L-Fucose-terminated glycoconjugates are recognized by pinocytosis receptors on macrophages. *Proc Natl Acad Sci USA* 78:1019-1022, 1981

35. ESPINOLA LG, BEAUCAIRE J, GOTTSCHALK A, et al: Radiolabeled liposomes as metabolic and scanning tracers in mice. II. In-111 oxine compared with Tc-99m DTPA, entrapped in multilamellar lipid vesicles. *J Nucl Med* 20: 434-440, 1979

1983 Conjoint Winter Congress
A Symposium on Emission Computed Tomography and Medical Data Processing

February 6-7, 1983 **Cathedral Hill Hotel** **San Francisco, California**

The Computer and Instrumentation Councils of the Society of Nuclear Medicine will meet February 6 and 7, 1983 at the Cathedral Hill Hotel in San Francisco, California.

In this meeting, the mechanics, the limitations, and the requirements of ECT will be discussed in depth. Along with technical papers, a few application papers will cover display and computer-based diagnosis. The meeting aims to be a forum for exchange and interaction, with ample time for questions, discussion, and debate. Technologists are cordially invited; you may register on-site.

Sunday, February 6

8:30 am	Opening Remarks Jon J. Erickson, PhD, Bryan Westerman, PhD, Michael L. Goris, MD, PhD
9:00	The Mathematical and Physical Basis of ECT
9:45	Comparison of SPECT Techniques on High-Speed Digital Array Processor
10:15	Coffee break
10:45	SPECT System Misalignment: Comparison of Phantom and Patient Images
11:15	Methods for Characterizing and Monitoring Rotational Gamma Camera's System Performance
11:45	Spatial/Temporal Dependency of Scintillation Camera Nonlinearization
12:15 pm	Lunch
1:45	An "Intelligent Assistant" for Hepatobiliary Imaging
2:10	Synthetic Color Composites of Related Images
2:30	The VEST—Validation of a Device for the Ambulatory Measurement of Ejection Fraction
3:00	Coffee break
3:30	Oblique Angle Display of ECT Images
4:00	Preliminary Characterization of Properties of a New Rotating SPECT Imaging System
4:30	Initial Experience with an Intelligent Gantry SPECT System

Monday, February 7

8:30 am	Attenuation Correction and Other Related Problems
9:45	The Orbiting Rod Source: Improving Performance in PET Transmission Correction Scans
10:15	Coffee break
10:45	Photon Attenuation in the Chest and an Empirical Correction Method in Myocardial SPECT Based on a Chest Phantom
11:15	Improving SPECT Image Quality by Body Contour Following
11:45	Appropriate Collimator for I-123 Imaging with SPECT
12:15 pm	Lunch
1:45	Decontamination of Time-Activity Curves from First-Pass Radionuclide Angiocardiographic Data
2:30	Measurement of Left Ventricular Volume Using Emission Computed Tomography
2:55	Experience with SPECT of the Liver
3:20	Coffee break
3:45	Limited Angle Tomography Using Rapid Digital Processing of Fresnel Zone Plate Data
4:15	Emission Computed Tomography: Versatile Limited Angle Software
4:45	Business meetings of the Computer and the Instrumentation Councils